NJC

Uranium extraction using magnetic CoFe2O4-graphene nanocomposite: Kinetics and thermodynamics studies

Journal:	*New Journal of Chemistry*
Manuscript ID:	NJ-ART-11-2014-001981.R1
Article Type:	Paper
Date Submitted by the Author:	23-Dec-2014
Complete List of Authors:	Tan, Lichao; Harbin Engineering University, Key Laboratory of Superlight Material and Surface Technology Liu, Qi; Harbin Engineering University, Song, Dalei; Harbin Engineering University, School of Material Science and Chemical Engineering jing, xiaoyan liu, jingyuan; harbin engineering university, college of material science and chemical engineering Li, Rumin; Harbin Engineering University, School of Material Science and Chemical Engineering hu, songxia; Institute of Advanced Marine Materials, Harbin Engineering University Liu, Lianhe; Harbin Engineering University, Wang, Jun; Harbin Engineering University, School of Material Science and Chemical Engineering

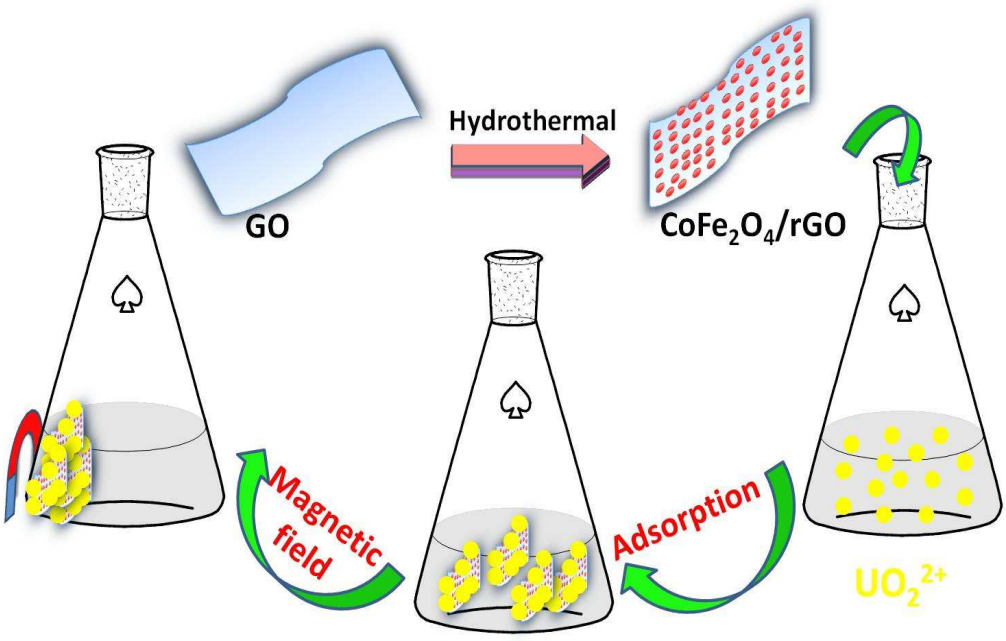
Hydrothermal
GO
$CoFe_2O_4$/rGO
Magnetic field
Adsorption
UO_2^{2+}

New Journal of Chemistry

Cite this: DOI: 10.1039/c0xx00000x

www.rsc.org/xxxxxx

ARTICLE TYPE

Uranium extraction using magnetic $CoFe_2O_4$-graphene nanocomposite: Kinetics and thermodynamics studies

Lichao Tan,[a] Qi Liu,*[a] Dalei Song,[a] Xiaoyan Jing,[a] Jingyuan Liu,[a] Rumin Li,[a] Songxia Hu,[b] Lianhe Liu,[b] and Jun Wang,*[a, b]

Received (in XXX, XXX) XthXXXXXXXXX 20XX, Accepted Xth XXXXXXXXX 20XX
DOI: 10.1039/b000000x

A novel magnetic nanocomposite($CoFe_2O_4$/rGO) consisting of reduced graphene oxide (rGO) and $CoFe_2O_4$ nanoparticles was fabricated. Scanning electron microscopy (SEM), transmission electron microscopy (TEM), X-ray diffraction (XRD) and vibrating sample magnetometer (VSM) were used to characterize the $CoFe_2O_4$/rGO. The as-obtained results indicate that $CoFe_2O_4$ nanoparticles have been successfully installed on the surface of rGO. Uranium adsorption (from synthetic solutions) has been investigated in batch systems. Moreover, the effects of different experimental parameters, such as initial solution pH (controlled with nitric acid), equilibration time, initial uranium concentration and temperature on sorption performance have been investigated. The results show that the kinetic data can be efficiently modelled using the pseudo-second-order equation. Furthermore, the Langmuir equation fits well sorption isotherms. In addition, the values of thermodynamic parameters ($\Delta G°$ and $\Delta H°$) show that the process is spontaneous and exothermic. Those experimental results exhibited a potential application of $CoFe_2O_4$/rGO in radionuclides cleanup.

Introduction

Hexavalent actinides constitute a significant ratio of radioactive species distribute nuclear wastes, which are generated in the post-processing process of spent fuels every year. Uranium isotopes are typical hazardous actinides with high radio toxicity as well as long half-lives. Due to the health and biological hazards that these elements represent, it is necessary that these hosts are resistant to radiation and environmental degradation over long time periods. Although various techniques for the removal of toxic and radiation metal ions have been developed, adsorption has been proved to be a more powerful technique for removing heavy metals pollutants as it is inexpensive, easy to perform and insensitive to toxic substances.[1, 2] Highly efficient adsorbents would enable the collection of trace-level metal ions from aqueous systems, thus improving the present technological level of radiation pollutant removal.[3]

Recently, the application of carbon-based nanomaterials in water treatment plants has attracted significant attentions for the advantages of large surface areas and more activated functionalized sites.[4, 5] Graphene is receiving intense attention, driven by its unique physical and chemical properties. As a result, graphene has been widely explored in a variety of applications including field-effect transistors, fuel cells, ultrasensitive sensors, electromechanical resonators, and supercapacitors, to name a few.[6] Graphene and graphene oxide have been reported as efficient adsorbents.[7] Yang et al. indicated that graphene oxide was proven to be a promising adsorbent for the decoloration of methylene blue (MB).[8] Deng et al. fabricated a functionalized graphene, which presents a high adsorption capacity for the removal of Pb (II) and Cd (II) from water.[9]

Over the years, magnetic adsorbents have emerged as a new generation of materials for environmental decontamination since magnetic separation simply involves applying an external magnetic field to extract the adsorbents.[10-14] Compared with traditional methods, such as filtration, centrifugation or gravitational separation, magnetic separation requires less energy and can achieve better separation especially for adsorbents with small particle size. Recently, ferrites have been employed in water purification. Glove et al. have reported adsorption of SO_2 by $CoFe_2O_4$ spinel ferrite nanoparticles and discussed corresponding magnetic changes.[15] The majority of magnetic adsorbent materials do not change in their magnetic properties upon adsorption; in addition, the unique response of magnetic nanoparticles to adsorbates allows them to serve as self-indicating adsorbents. Consequently, some researchers have managed to fabricate magnetic graphene nanocomposites. The $CoFe_2O_4$/rGO nanocomposites possess attractive properties which could see potential use in catalysis, biomedicine and lithium-ion batteries. However, there have been no reports on using $CoFe_2O_4$/rGO nanocomposite as a sorbent for uranium (U) or other actinides.

Herein, we demonstrate a facile hydrothermal method to fabricate a $CoFe_2O_4$/rGO nanocomposite. The prepared samples were characterized by XRD, SEM, TEM and magnetic measurements. To investigate the adsorption of $CoFe_2O_4$/rGO, the uranium (VI) was selected as the model compound. Furthermore, we demonstrated that $CoFe_2O_4$/rGO nanocomposites have great potential as an effective absorbent for removing uranium (VI) in water, due to its convenient magnetic separation and high adsorption capacity.

Experimental

Synthesis of the $CoFe_2O_4$/rGOnanocomposite

The graphene oxide (GO) was obtained according to the previous report.[16] Using an ultrasonication method exfoliated GO, 10 mg mL^{-1} GO aqueous suspension was prepared by dispersing the graphene oxide in deionized water. Firstly, 2 mmol of $FeSO_4 \cdot 7H_2O$ and 1 mmol of $CoCl_2 \cdot 4H_2O$ were dissolved in a mixture of 30 mL of ethylene glycol and 20 mL of distilled water. Then, appropriate amount of GO aqueous and 2 mL of ammonia solution were added to the mixture with stirring for 1 h. The resulting solution was then poured into a 100 mL Teflon-lined autoclave and heated to180 ^oC, and kept at that temperature for 24 h. After cooling to room temperature, the precipitate was collected by magnet and washed repeatedly with distilled water and ethanol; it was then dried for12h at 60 ^oC.

Adsorption experiments

In a typical experiment, 0.02 g of $CoFe_2O_4$/rGO nanocomposite was mixed with 50mL of $UO_2(NO_3)_2 \cdot 6H_2O$ solution. After the adsorption processes, the samples were isolated from the supernatant by use of a magnet, and the supernatant solutions were analyzed with WGJ–III Trace Uranium Analyzer to obtain the concentrations of uranium (VI) in solution. The solution pH was adjusted by addition of 0.5 M HNO_3 and NaOH. The amount of uranium (VI) adsorbed per unit mass of the adsorbent was calculated according to Eq. (1):

$$Q_e = (C_0 - C_e) \cdot V / m \quad (1)$$

where Q_e is the adsorption capacity of adsorbent, C_0 and C_e (mg L^{-1}) are concentration of uranium (VI) at the initial and equilibrium states, respectively, V (L)is the volume of the solution and m is the weight of sorbent (g).

Characterization

Crystallite structures were determined by X-ray diffraction (XRD) using a Rigaku D/max-IIIB diffractometer with Cu Kα irradiation (λ=1.54178 Å). Raman spectra were acquired on a LabRAM HR Evolution in Via Reflex Raman Microprobe. The X-ray source was operated at 40 kV and 150 mA. The morphology was characterized using transmission electron microscopy (TEM, FEI Tecnai G^2 20 S–TWIN) and a scanning electron microscope (SEM, JSM-6480A, Japan Electronics). The magnetic measurement was carried out with a vibrating sample magnetometer (VSM, Lanzhou University Lake Shore 7304). Effluent was analyzed using WGJ–III Trace Uranium Analyzer from the Company of Hangzhou Daji Photoelectric Instrument.

Results and discussions

Characterization of samples

Fig. 1 shows the XRD patterns of as-synthesized GO, rGO, $CoFe_2O_4$ and $CoFe_2O_4$/rGO, respectively. In the XRD pattern of GO (Fig. 1a), we can see a sharp diffraction peak at 10.8°, which is assigned to GO. The (001) interlayer spacing of the as-obtained exfoliated GO is calculated to be 0.82 nm, showing an complete oxidation of graphite to the graphite oxide due to the introduction of oxygen-containing functional groups on the graphite sheets.[17] After hydrothermal treatment, the peak at 10.8° completely disappears and a broad peak corresponding to rGO at about 24.5° with an interlayer spacing of 0.363 nm is observed (Fig. 1b), which is a little larger than the spacing for natural graphite (0.34 nm). For pure $CoFe_2O_4$ (Fig. 1c), all diffraction peaks from the XRD pattern of the pure $CoFe_2O_4$ can be indexed to the $CoFe_2O_4$ spinel with Fd3 m space group (JCPDS No. 22-1086). For the $CoFe_2O_4$/rGO nanocomposite (Fig. 1d), there is a large hump at about 25° for the XRD pattern of the $CoFe_2O_4$/rGO nanocomposite, which can be attributed to the grapheme (002) peak. The five main characteristic diffraction peaks at 30.1°, 35.4°, 43.1°, 57.0° and 62.6° can be assigned to (220), (311), (400), (511) and (440) planes of $CoFe_2O_4$, which is in good conformity with standard power diffraction patterns of $CoFe_2O_4$ with the lattice constants. It indicates that hybrid materials synchronously possess the characteristic diffraction peaks of $CoFe_2O_4$ aggregates.

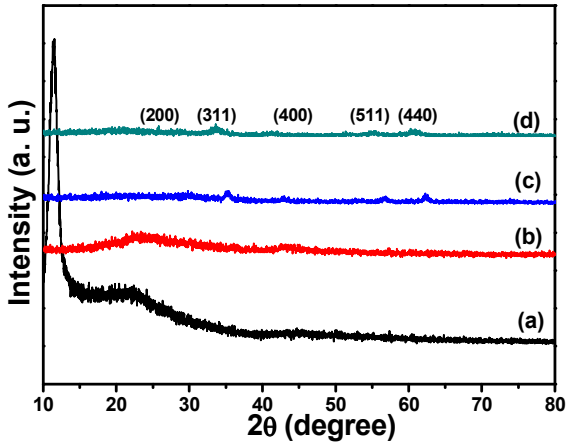

Figure1. XRD patterns of as-synthesized GO, rGO, $CoFe_2O_4$ and $CoFe_2O_4$/rGO.

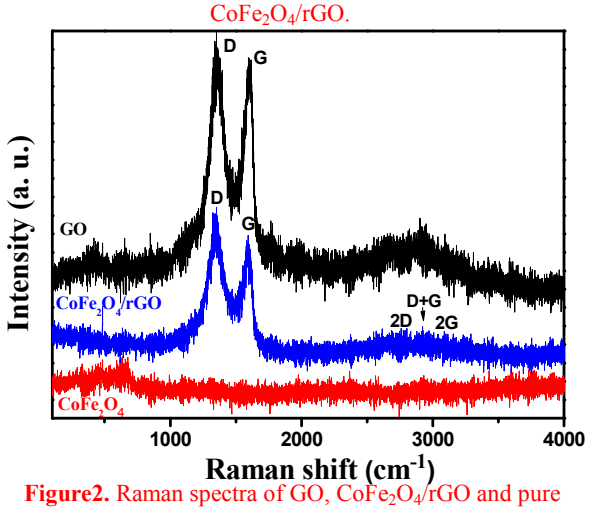

Figure2. Raman spectra of GO, $CoFe_2O_4$/rGO and pure $CoFe_2O_4$.

Raman spectroscopy is also one of the most sensitive and informative techniques to characterize disorder in sp^2 carbon materials. As shown in Fig. 2, for $CoFe_2O_4$/rGO, Raman peaks of G- and D- bands shift to lower frequency in comparison with that of GO: the G-band shifted from 1602 to 1589 cm^{-1}, whereas the D-band shifted from 1362 to 1346 cm^{-1}, indicating that GO has been reduced to graphene.[18, 19] Additionally, the 2D band at 2696 cm^{-1} is also observed, which is further indicative of the reduction

of GO and the formation of graphene. The peak position of the 2D band is similar to that of monolayer graphene.[20, 21] The two Raman spectra of $CoFe_2O_4$/rGO and pure $CoFe_2O_4$ show similar features in the frequency range between 100 and 1000 cm^{-1} as reported in literatures for spinel $CoFe_2O_4$, indicating the formation of spinel $CoFe_2O_4$ phase during the hydrothermal treatment. [22]

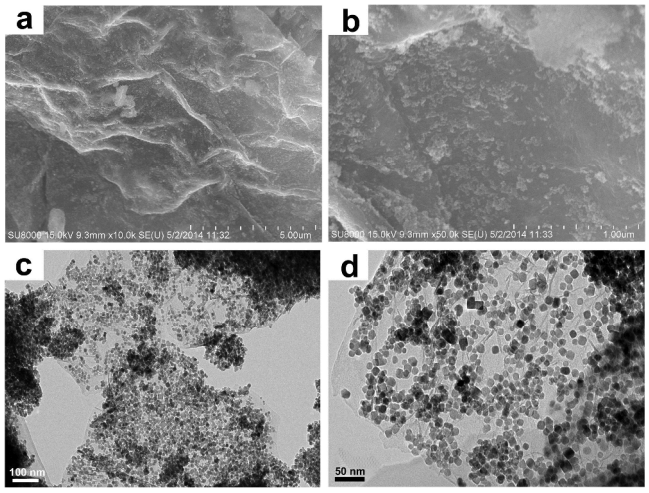

Figure3. Representative SEM images of $CoFe_2O_4$/rGO (a) and (b); TEM images of $CoFe_2O_4$/rGO (c) and (d).

The typical morphology of the $CoFe_2O_4$/rGO nanocomposite was characterized by SEM and TEM. Fig. 3A, B show the SEM images of the $CoFe_2O_4$/rGO nanocomposite. It can be seen that $CoFe_2O_4$ nanoparticles uniformly disperse on the surface of graphene sheets and between the layers of graphene sheets. The details of $CoFe_2O_4$/rGO have been further examined by TEM. Fig. 3C and D shows that the size of $CoFe_2O_4$ particles ranges 5–40 nm, and the $CoFe_2O_4$ particles uniformly disperse on graphene sheets.

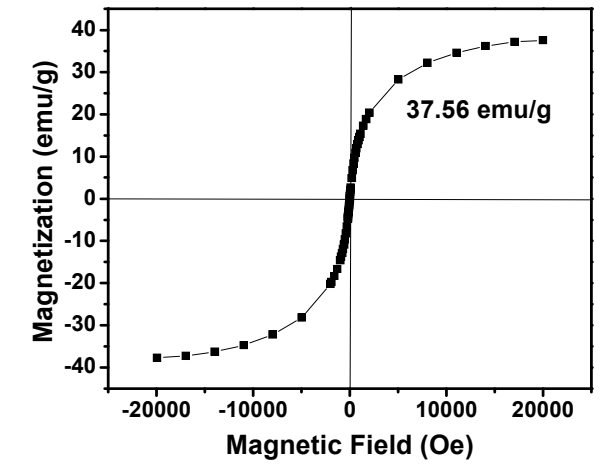

Figure4. Magnetic hysteresis curve for $CoFe_2O_4$/rGO.

The magnetization curves of $CoFe_2O_4$/rGO tested at 300 K are depicted in Fig. 4. The negligible coercivity or remanence indicates that $CoFe_2O_4$/rGO exhibits super paramagnetic behavior. The specific saturation magnetization is 37.56 emu g^{-1}. Importantly, a large saturation magnetization makes this adsorbent easy to separate from solution by applying an external magnetic field.

Adsorption Experiments

Effect of solution pH

The effect of initial pH of the uranium solution on the adsorption was systematically investigated over a pH range from 2.0 to 12.0. The variation of the uranium adsorption capacity with initial pH is shown in Fig. 5. From Fig. 5, we found the fact that the uranium (VI) ions adsorption strongly depends on the pH of solution. The adsorption capacity sharply increases when the pH increases from 2.0 to 6.0. The maximum adsorption capacity is observed at pH 6.0. In acidic conditions, uranium (VI) is present in solution predominantly in the form of UO_2^{2+} and the sorption is low because of the competition of H^+ ions for the binding sites of the adsorbents. The adsorption capacity diminished as pH continued to rise from 6.0 to 12.0. As the pH increased, hydroxyl, dissolved carbonate and bicarbonate anions also increased. Therefore, the uranyl ion forms stable complexes with hydroxyl and carbonate, which lead to a sharp decrease in adsorption capacity.[23] As a consequence, pH 6.0 is considered as the optimum pH for further experiments.

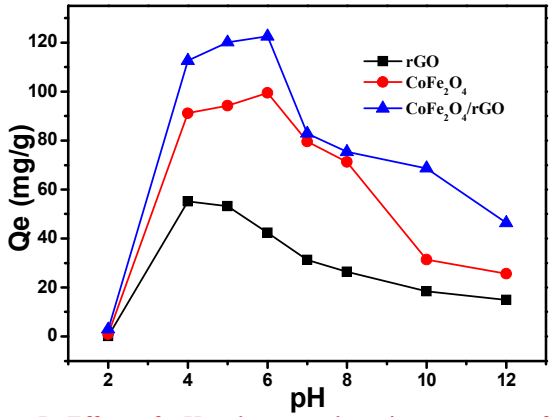

Figure5. Effect of pH value on adsorption property of pure $CoFe_2O_4$, rGO and $CoFe_2O_4$/rGO. pH 2.0-12.0; temperature 25°C; amount of $CoFe_2O_4$/rGO 0.02 g.

The adsorption of uranium (VI) onto rGO, $CoFe_2O_4$ and $CoFe_2O_4$/rGO was carried out by varying pH in the range of 2.0−12.0 (Fig. 5). rGO shows low adsorption capacity for uranium, indicating that rGO has a rare contribution for uranium removal in the composite. In contrast, $CoFe_2O_4$ and $CoFe_2O_4$/rGO have high adsorption capacity for uranium, meaning that $CoFe_2O_4$ mostly contribute to uranium removal in the composite. $CoFe_2O_4$/rGO shows high adsorption capacity for uranium, indicating this uniquely structured composite are favorable for achieving high adsorption performance.

Effect of contact time and adsorption dynamics

Sorption kinetics is one of the most important characteristics for solid-phase extraction, which demonstrates the sorption efficiency of adsorbents. The effect of the contact time on uranium (VI) sorption on $CoFe_2O_4$/rGO is depicted in Fig. 6. As can be seen, the amount of uranium (VI) sorption increased rapidly in the first 120 min of contact time and thereafter it proceeded at a slow rate and finally reached equilibrium at 180 min. Therefore, the contact time was set to 240 min in future

experiments to ensure each adsorption equilibrium is achieved. As a result, a maximum equilibrium capacity of 126.5 mg g^{-1} is obtained with an initial uranium (VI) solution of 50 mg L^{-1}.

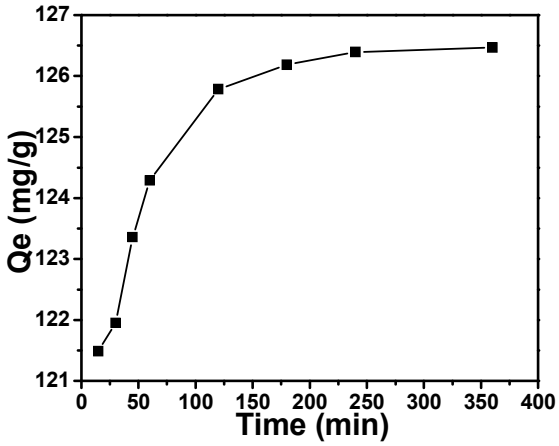

Figure6. Effect of contact time on uranium (VI) adsorption. pH 6.0; temperature 25 °C; amount of $CoFe_2O_4$/rGO 0.02 g

Table 1 Pseudo-first-order and pseudo-second-order constants and values of R^2 for $CoFe_2O_4$/rGO.

Kinetic model	T (°C)	C_0 (mg/L)	$Q_{e,exp}$ (mg/g)	$Q_{e,cal}$ (mg/g)	k_1(min^{-1})/k_2 (g/mg·min)	R^2
Pseudo-first order	25	50	126.5	5.677	0.0151	0.9796
Pseudo-secondorder	25	50	126.5	125.2	0.0073	0.9999

Utilization of appropriate kinetic models can offer useful information for understanding the underlying sorption mechanisms. From this aspect, the experimental sorption data have been fitted using pseudo-first-order and pseudo-second-order kinetic models. The pseudo-first-order kinetic model describes the sorption process based on sorbent capacity and can be written as: [24-26]

$$ln(q_e - q_t) = ln(q_e) - k_1 t \quad (2)$$

The pseudo-second-order model considers the whole sorption process including external film diffusion, sorption, and internal particle diffusion, and can be written as:

$$\frac{t}{q_t} = \frac{1}{k^2 \cdot q_e^2} + \frac{t}{q_e} \quad (3)$$

where q_e and q_t are the sorption amounts of uranium (VI) (mg L^{-1}) at equilibrium time (h) and time t (h), respectively; k_1 (min^{-1}) and k_2 (g mg^{-1} min^{-1}) represent the kinetic rate constants of the pseudo-first-order and pseudo-second-order models, respectively. From the linear plot of ln (q_e-q_t) vs t (Figure 7A), the k_1 and theoretical q_e values ($q_{e,cal}$) of the pseudo-first-order model are obtained. And from the linear plot of t/q_t vs t (Figure 7B), the $q_{e,cal}$ and k_2 values of the pseudo-second-order model are obtained. The calculated kinetic parameters from both model fittings are shown in Table 1. Since the correlation coefficient for pseudo-second-order kinetics model is found to closer to unity than that for pseudo-first-order kinetic model, it can be inferred that the sorption kinetics of uranium (VI) could be explained well in terms of pseudo-second-order kinetic model for the $CoFe_2O_4$/rGO adsorbents.

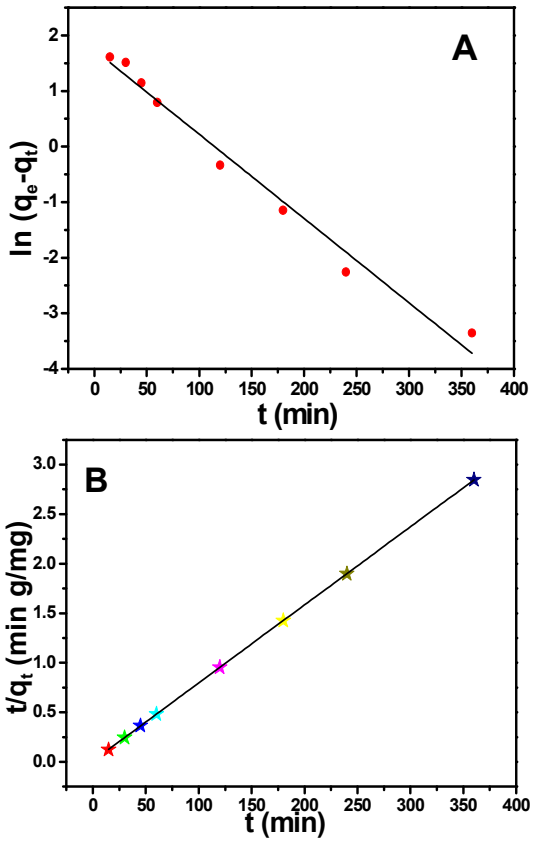

Figure7. Pseudo-first-order (A), pseudo-second-order (B) plot for the removal of uranium (VI) by $CoFe_2O_4$/rGO. pH 6.0; temperature 25 °C; amount of $CoFe_2O_4$/rGO 0.02 g.

Effect of temperature and adsorption thermodynamics

The adsorption experiments at different temperatures were also performed to evaluate the influence of temperature (25-55 °C) as shown in Figure8. The results show that the adsorption of uranium (VI) is favored with an increase of temperature.

The temperature dependence of adsorption process is associated with changes in several thermodynamic parameters such as standard free energy ($\Delta G°$), enthalpy ($\Delta H°$) and entropy ($\Delta S°$) of adsorption, which are calculated by equations (4) and (5).[27]

$$lnK_d = -\Delta H^0 / RT + \Delta S^0 / R \quad (4)$$

where K_d is the equilibrium constant (mL g^{-1}), $\Delta H°$ is the standard enthalpy (KJ mol^{-1}), $\Delta S°$ is the standard entropy (J mol^{-1} K^{-1}), T is the absolute temperature (K), and R is the gas constant (8.314 J mol^{-1} K^{-1}). The values of $\Delta H°$ and $\Delta S°$ are evaluated from the intercept and slope of the linear plot of ln K_d vs. $1/T$ (Fig. 9).

The thermodynamic parameter, $\Delta G°$, is calculated from the following Gibbs-Helmholtz equation:

$$\Delta G^0 = \Delta H^0 - T \cdot \Delta S^0 \quad (5)$$

where $\Delta G°$ is the standard free energy (KJ mol^{-1}).The calculated values of $\Delta G°$, $\Delta H°$ and $\Delta S°$ under different temperatures are

presented in Table 2. The positive values of $\Delta H°$ confirm the endothermic nature adsorption. The positive standard entropy ($\Delta S°$) indicates the increased randomness at the solid/liquid interface during the adsorption of uranium (VI) on $CoFe_2O_4$/rGO. The negative values of $\Delta G°$ indicate that the adsorption follows a feasible and spontaneous trend. Notably, the values of $\Delta G°$ become more negative with the increase in temperature, indicating that the higher temperature may facilitate adsorption uranium (VI) on $CoFe_2O_4$/rGO due to a greater driving force of adsorption.

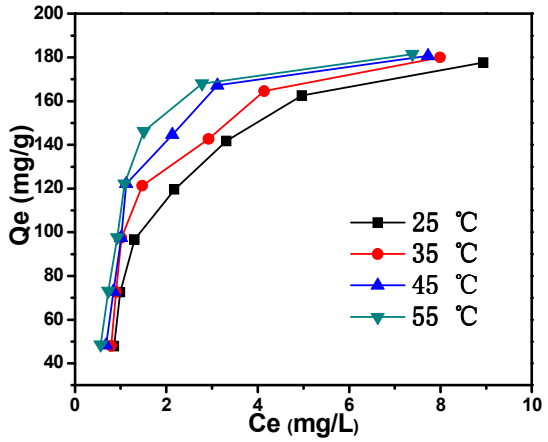

Figure8. Adsorption isotherm of $CoFe_2O_4$/rGO for uranium (VI) at different temperatures. pH 6.0; temperature 25-55 °C; amount of $CoFe_2O_4$/rGO 0.02 g.

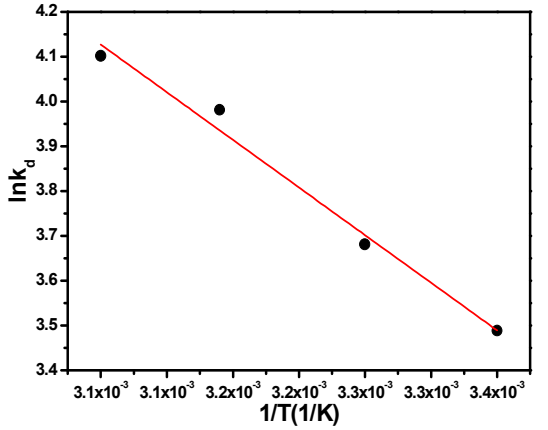

Figure9. Relationship curve between $\ln K_d$ and 1/T.

Table 2 Thermodynamics parameters for uranium adsorption on $CoFe_2O_4$/rGO.

$\Delta H°$	$\Delta S°$	$\Delta G°$			
(kJ mol^{-1})	(J mol^{-1}·K^{-1})	(kJ mol^{-1})			
		298K	308K	318K	328K
17.68	88.21	-8.69	-9.57	-10.45	-11.33

Adsorption isotherms of uranium

To understand the effect of initial UO_2^{2+} concentration on sorption capacity of the adsorbent, the sorption isotherms of UO_2^{2+} on the investigated composite at different UO_2^{2+} concentration are shown in Fig. 8. Obviously, increasing the UO_2^{2+} concentrations involves an increase in the uptake of UO_2^{2+}. The sorption isotherm is the most important information, which indicates how the sorbent molecules distribute between the solid and the liquid phase when the sorption process reaches an equilibrium state.

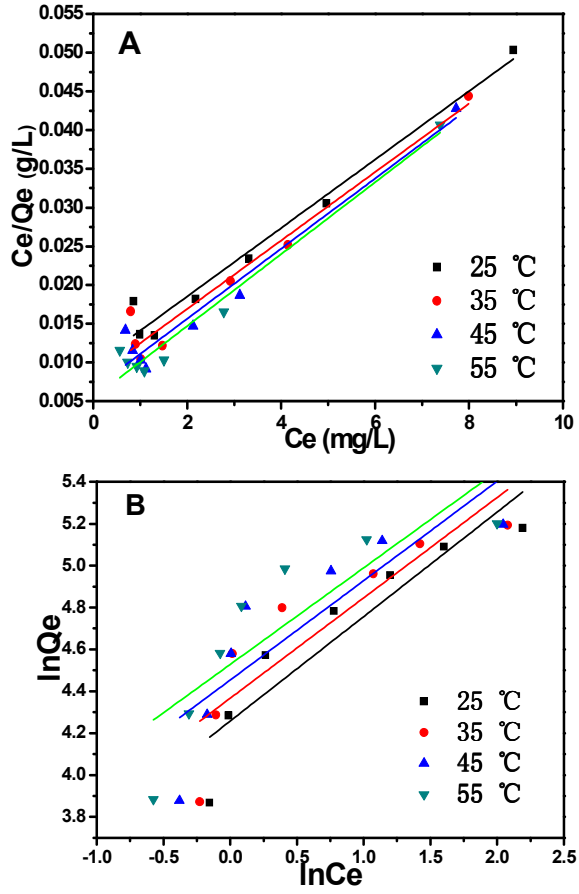

Figure10. Comparison of the model fits of Langmuir (A) and Freundlich (B) for the removal of uranium (VI) by $CoFe_2O_4$/rGO. pH 6.0; temperature 25-55 °C; amount of $CoFe_2O_4$/rGO 0.02 g.

To understand the sorption behavior, the adsorption equilibrium data have been analyzed using various isotherm models,[28] such as the Langmuir, the Freundlich equations. The linearized form of the Langmuir equation is given by Eq. 6:

$$C_e / q_e = 1/b \cdot q_m + C_e / q_m \quad (6)$$

where C_e (mg L^{-1}) is the solute equilibrium concentration, q_e (mg g^{-1}) is the amount of solution adsorbed per unit mass of the adsorbent, q_m is the maximum adsorption capacity (mg g^{-1}), b is Langmuir constant. According to Eq. (6), a straight line is obtained and presented in Fig. 10A. The values of q_m and b are calculated from the slope and the intercept and the results are given in Table3.

Freundlich isotherm model is based on the assumption of an exponentially decaying adsorption site energy distribution.[28, 29] It is applied to describe heterogeneous system and this is characterized by the heterogeneity factor, n. The linearized form

of the Freundlich equation is given by Eq. 7:

$$lnq_e = lnk + \frac{1}{n} lnC_e \quad (7)$$

where k and n are the Freundlich constants related to the adsorption capacity and adsorption intensity, respectively. They are determined from the intercept and slope of the linear plot of $\ln q_e$ versus $\ln C_e$ (Fig. 10B).

Table 3 reports that the Langmuir isotherm model fits well with the experimental results over the experimental range, with high correlation coefficients (>0.94). According to the Langmuir isotherm, monolayer saturation capacity of 227.2 mg g^{-1} for uranium (VI) for $CoFe_2O_4$/rGO can be obtained at 25 °C.

Table 3 Isotherm constants and values of R^2 for $CoFe_2O_4$/rGO.

T(K)	Langmuir isotherm			Freundlich isotherm		
	Q_m (mg g^{-1})	b (L mg^{-1})	R^2	K (L g^{-1})	n	R^2
298	227.2	0.454	0.9669	70.59	2.004	0.8279
308	227.2	0.543	0.9457	78.81	2.086	0.7427
318	222.2	0.682	0.9467	85.88	2.107	0.6831
328	217.4	0.852	0.9617	92.57	2.168	0.6788

Conclusions

In conclusion, a novel magnetic $CoFe_2O_4$/rGO composite has been fabricated, with its structure well-characterized by XRD, SEM, TEM and VSM. The $CoFe_2O_4$/rGO exhibited higher adsorption efficiency in removing uranium (VI) from aqueous solution and the adsorption process was pH dependence. Moreover, the adsorption process is accomplished within 240 min and the adsorption kinetic process can be well described by the pseudo-second-order model. Thermodynamic studies indicate an endothermic and spontaneous adsorption process. In addition, uranium (VI)-loaded $CoFe_2O_4$/rGO is easily separated from aqueous solutions by a magnet. The easy operation and fast and efficient sorption performance indicate that $CoFe_2O_4$/rGO can be used as a highly effective material for the removal and recovery of uranium (VI) from water.

Acknowledgements

This work was supported by National Natural Science Foundation of China (21353003), Special Innovation Talents of Harbin Science and Technology (2013RFQXJ145), Fundamental Research Funds of the Central University (HEUCFZ), Natural Science Foundation of Heilongjiang Province (B201316), Program of International S&T Cooperation special project (2013DFR50060), and the fund for Transformation of Scientific and Technological Achievements of Harbin (2013DB4BG011), Research and Development of Industrial Technology Project of Jilin Province (JF2012C022-4)

Notes and references

[a] *Key Laboratory of Superlight Material and Surface Technology, Ministry of Education, Harbin Engineering University, Harbin 150001, China. Tel. +86 451 8253 3026; fax: +86 451 8253 3026.*
E-mail address: zhqw1888@sohu.com
[b] *Institute of Advanced Marine Materials, Harbin Engineering University, 150001, China.*

1. Z. Sun, C. Li, D. Wu, J. Chem. Technol. Biotechnol. 2010, 85, 845-850.
2. M. Asadullah, M. Asaduzzaman, M.S. Kabir, M.G. Mostofa, T. Miyazawa, J. Hazard. Mater. 2010, 174, 437-443.
3. J.L. Wang, C. Chen, Bioresource Technology. 2014,160, 129–141
4. G.S. Situate, S.G. lyuke, S. Ndlovu, M. Heydenrych, Water Res. 2012, 46, 1185-1197.
5. G. Zhao, J. Li, X. Ren, C. Chen, X. Wang, Pnviron. Sci Technol. 2011, 45, 10454-10462.
6. M. J. Allen, V. C. Tung, R. B. Kaner, Chem. Rev. 2009, 110 (1), 132-145.
7. G. Jung, Z. Lin, C. Chen, L. Zhu, Q. Chang, N. Wang, W. Wei, H. Tang, Carbon. 2011, 49, 2693-2701.
8. S. Yang, S. Chen, Y. Chang, A. Cao, Y. Liu, H. Wang, J. Colloid Interface Sci. 2011, 359, 24-29
9. X. Deny, L. Lv, H. Li, F. Luo, J. Hazard. Mater. 2010, l83, 923-930.
10. P. Wang, Q. Shi, Y. Shi, K.K. Clark, G.D. Stucky, A.A. Keller, J. Am. Chem. Soc. 2009, 131, 182-188.
11. Z. Sun, L. Wang, P. Liu, S. Wang, B. Sun, D. Jiang, F. Xiao, Adv. Mater. 2006, 18, 1968-1971.
12. J. Hu, L. Zhong, W. Song, L. Wan, Adv. Mater. 2008, 20, 2977-2982.
13. V. Rocher, A. Bee, J.M. Siaugue, V. Cabuil, J. Hazard. Mater. 2010, 178, 434-439.
14. Y.M. Zhai, J.F. Zhai, M. Zhou, S.J. Dong, J. Mater. Chem. 2009, 19, 7030-7035.
15. T.G. Glover, D. Saho, L.A. Vaughan, J.A. Rossin, Z.J. Zhang, Langmuir. 2012, 28, 5695-5702.
16. W. S. Hummers and R. E. Offeman, J. Am. Chem. Soc. 1958, 80, 1339.
17. J. L. Gunjakar, I. Y. Kim, J. M. Lee, N.-S. Lee and S.-J. Hwang, Energy Environ. Sci. 2013, 6, 1008.
18. S. Stankovich, D.A. Dikin, R.D. Piner, K.A. Kohlhaas, A. Kleinhammes, Y. Jia, Y. Wu, S.T. Nguyen, R.S. Ruoff, Carbon. 2007, 45, 1558–1565.
19. T.N. Lambert, C.A. Chavez, B. Hernandez-Sanchez, P. Lu, N.S. Bell, A. Ambrosini, T. Friedman, T.J. Boyle, D.R. Wheeler, D.L. Huber, J. Phys. Chem. C 2009, 113, 19812–19823.
20. K.S. Vasu, B. Chakraborty, S. Sampath, A.K. Sood, Solid State Commun. 2010, 150, 1295–1298.
21. S.C. Ray, A. Saha, S.K. Basiruddin, S.S. Roy, N.R. Jana, Diamond Relat. Mater. 2011, 20, 449–453.
22. H. Xia, D.D. Zhu, Y.S. Fu, X. Wang, Electrochimica Acta. 2012, 83, 166–174.
23. G. Wang, J. Liu, X. Wang, Z. Xie, N. Deng, J. Hazard. Mater. 2009, 168, 1053-1058.
24. Y. S. Ho, G. McKay, Water. Res. 2000, 34, 735.
25. J. Yu, H. B. Bai, J. Wang, Z. S. Li, C. S. Jiao, Q. Liu, M. L. Zhang, L. H. Liu, New. J. Chem. 2013, 37, 366.

26. Y. Miyake, H. Ishida, S. Tanaka, D. Kolev, Chem. Eng. J. 2013, 218, 350.
27. K.Y. Foo, B.H. Hameed, Chem. Eng. J. 2010,156, 2-10.
28. H.M.F. Freundlich, Z. Phys. Chem. 1906, 57, 385-470.
29. M.S. Sajab, C.H. Chia, S. Zakaria, S.M. Jani, M.K. Ayob, K.L. Chee, P.S. Khiew, Bioresour Technol. 2011, 102, 7237–7243.

Table of Contents

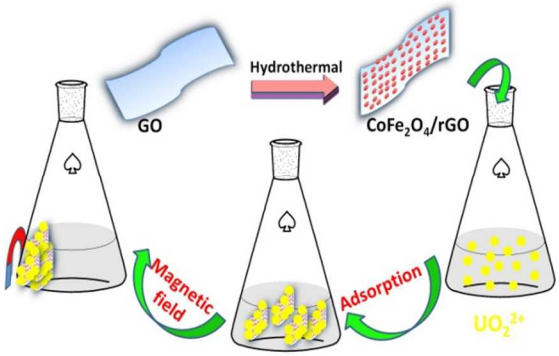

$CoFe_2O_4$/rGO was prepared and exhibited fast and efficient sorption for uranium (VI).